

## 8.1 Introduction

In Section 5.2 and Chapter 7 we discussed the global annual cycle in the mean zonal wind and temperature fields. This cycle is roughly antisymmetric with respect to the equator and, although dominant in the extratropics, has relatively little amplitude in equatorial latitudes. In the equatorial middle atmosphere above 35 km the seasonal variation is characterized primarily by a *semiannual* oscillation of the mean zonal wind. Well below 35 km, on the other hand, the equatorial stratospheric seasonal cycle is completely overwhelmed by a long-term oscillation that is not directly linked to the march of the seasons. This oscillation, which is of somewhat irregular period (averaging 27 months), is called the “quasi-biennial” oscillation (QBO).

The annual cycle in the mean zonal wind is fundamentally driven by the annual cycle in solar insolation. As shown in Chapter 7, in the extratropical stratosphere, eddy forcing acts primarily to warm the winter polar regions and hence damp the amplitude of the response to radiative driving. Since the sun passes overhead twice per year in the equatorial zone, radiative heating in that region has a significant semiannual component. Thus, it is not surprising that by analogy with the annual cycle efforts to explain the semiannual wind oscillation at first focused on thermal forcing. Despite the irregularity of the period of the QBO, early theoretical attempts to account for that oscillation also invoked thermal forcing mechanisms.

However, oscillating thermal forcing, in the absence of eddies, is far less effective in generating an oscillating mean zonal temperature and wind response in equatorial regions than at higher latitudes. For low latitudes,

taking  $f_0 = O(\beta L)$ , where  $L$  is a typical meridional scale for the mean flow ( $\sim 1200$  km) and  $\beta$  takes its equatorial value  $2\Omega/a$ , we have

$$f_0^2 L^2 / N^2 H^2 = O(\beta^2 L^4 / N^2 H^2) = O(10^{-2}).$$

In this case the scaling argument described in Section 7.2.2 gives

$$\frac{\partial \bar{T}}{\partial t} \sim (\bar{T} - T_r) / \tau_e,$$

in place of Eq. (7.2.8), where  $\tau_e \equiv (N^2 H^2 / \beta^2 L^4) \tau_r = O(10^2 \tau_r)$ . If  $\tau_r$  is a few days, then  $\tau_e$  is much greater than the seasonal timescale  $\tau \sim 3$  months. The amplitude  $\Delta \bar{T}$  of the associated oscillation in  $\bar{T}$  will thus be much smaller [by a factor  $O(\tau / \tau_e)$ ] than the amplitude  $\Delta T_r$  of the oscillation of  $T_r$  in a purely radiative model, rather than the same magnitude as at high latitudes. The amplitude of the corresponding oscillation in  $\bar{u}$  can be estimated from Eq. (7.2.1d) as

$$\Delta \bar{u} \sim \left( \frac{R \Delta \bar{T}}{f_0 L} \right) \sim \left( \frac{R \Delta \bar{T}}{\beta L^2} \right),$$

which is  $O(\tau / \tau_e)$  smaller than  $\Delta u_r \sim R \Delta T_r / \beta L^2$ , rather than the same order, as in the extratropics. This argument, which is supported by detailed calculations, indicates that it is very difficult to drive mean zonal temperature and wind oscillations in the equatorial region by thermal forcing alone. For the equatorial quasi-biennial and semiannual oscillations, wave driving must be considered the primary forcing.

## 8.2 The Observed Structure of the Equatorial Quasi-Biennial Oscillation

The equatorial QBO was originally discovered in 1960 by Reed and independently by Veryard and Ebdon (Reed *et al.*, 1961; Veryard and Ebdon, 1961). Many of the essential dynamical aspects of the QBO are best displayed by time-height sections showing the departure of the monthly averaged mean zonal wind from its long-term monthly mean at equatorial stations. The example shown in Fig. 8.1 clearly illustrates the following features:

1. An alternating pattern of eastward and westward wind regimes that repeat at intervals varying from about 22 to 34 months, with an average period of about 27 months.
2. Downward propagation of successive regimes at an average rate of about 1 km/month, but with westerly shear zones descending more regularly and more rapidly than easterly shear zones.

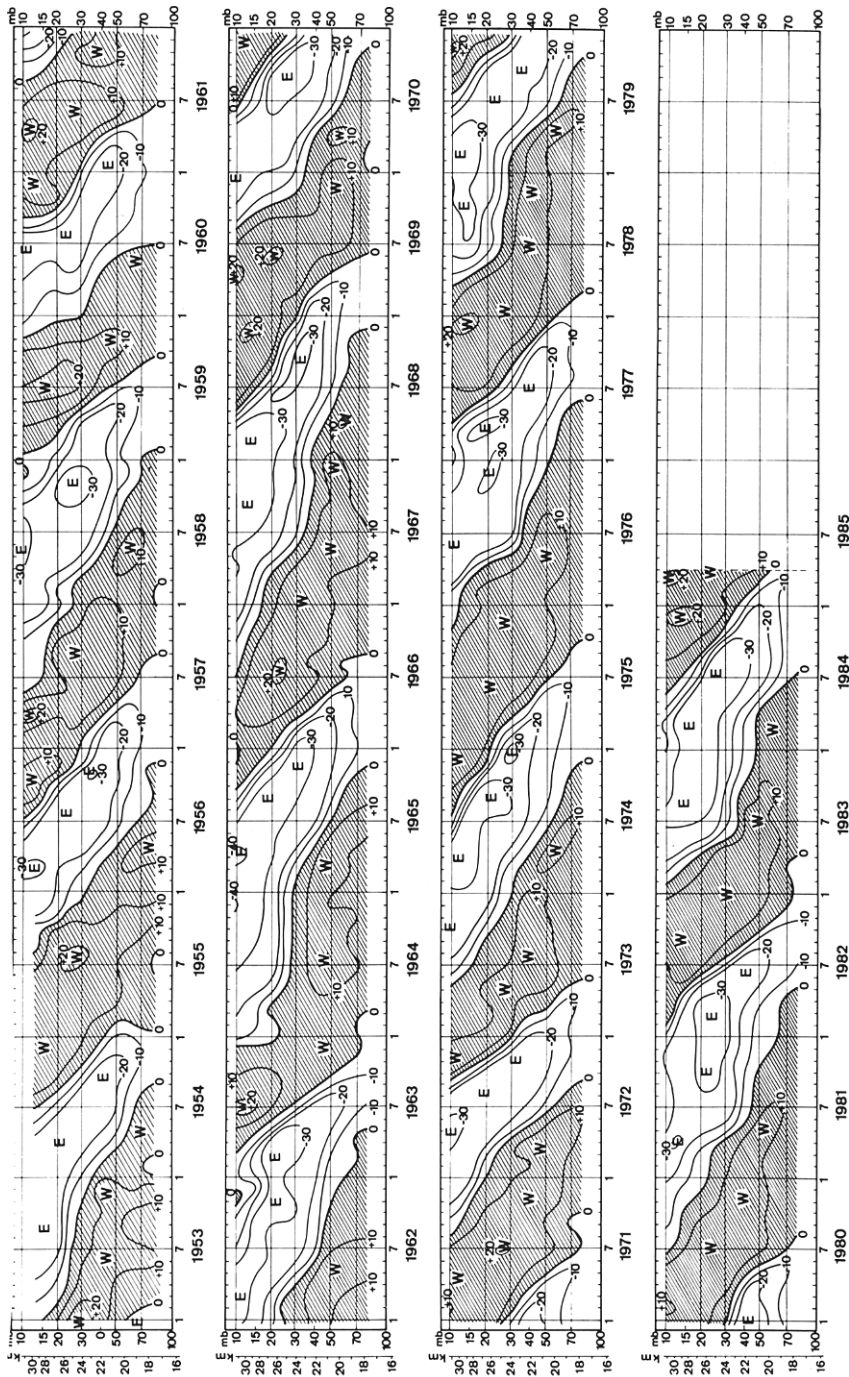


Fig. 8.1. Time-height section of monthly mean zonal winds ( $\text{m s}^{-1}$ ) at equatorial stations (Jan. 1953–Aug. 1967: Canton Island,  $3^{\circ}\text{S}/172^{\circ}\text{W}$ ; Sept. 1967–Dec. 1975: Gan/Maldives Islands,  $1^{\circ}\text{S}/73^{\circ}\text{E}$ ; Jan. 1976–Apr. 1985: Singapore,  $1^{\circ}\text{N}/104^{\circ}\text{E}$ ). Isotherms are at  $10\text{-m s}^{-1}$  intervals. Note the alternating downward propagating westerly (W) and easterly (E) regimes. [From Naujokat (1986), with permission.]

3. Amplitude nearly constant in height between about 40 and 10 mb, but decreasing rapidly as regimes descend below the 50 mb level.

The last of these features is further illustrated by the latitude–height section of amplitude and phase shown in Fig. 8.2. The oscillation has an approximate Gaussian distribution about the equator with a latitudinal half-width of about 12 degrees. There is very little phase dependence on latitude.

A closer examination of the latitude–time dependence of the QBO does, however, reveal some remarkable asymmetries between the westerly and easterly acceleration phases. As shown in Fig. 8.3 at 30 mb, westerly accelerations appear first at the equator and spread to higher latitudes, while the easterly accelerations are rather more uniform in latitude. The westerly accelerations are more intense on average than the easterly, consistent with the more rapid descent of the westerly shear zone.

Although the QBO is definitely not a 2-year oscillation, there appears to be a tendency for a seasonal preference in the phase reversal so that, for example, the onset of both westerlies and easterlies occurs mainly during Northern Hemisphere summer at the 50 mb level (see Figs. 8.1 and 8.4).

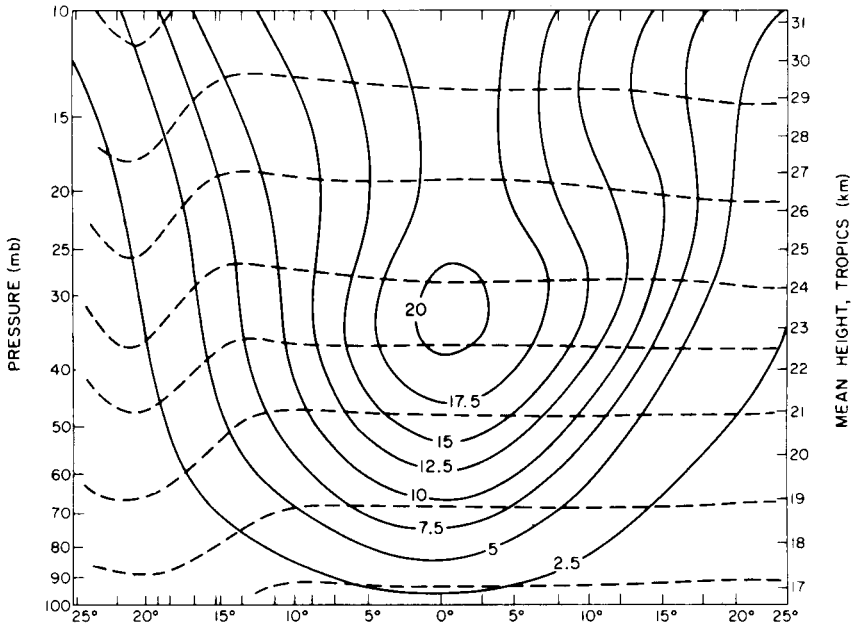


**Fig. 8.2.** Latitude–height distribution of the amplitude and phase of the zonal wind QBO. Amplitude (solid lines) in  $\text{m s}^{-1}$ , phase (dashed lines) at 1-month intervals with time increasing downward. [From Wallace (1973), with permission, adapted from an original drawing by R. J. Reed.]

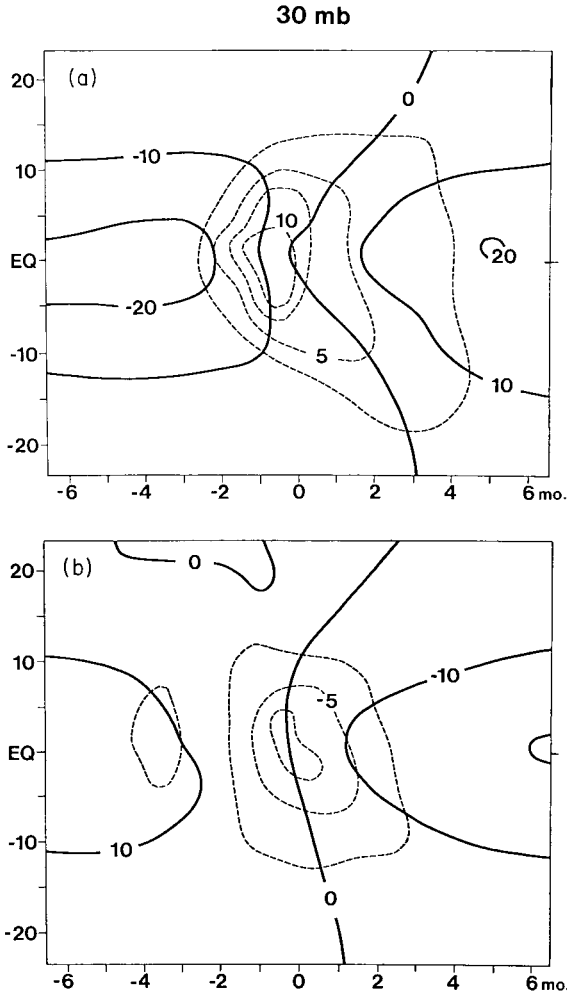


**Fig. 8.3.** Composite latitude-time section of zonal wind at 30-mb for westerly (upper) and easterly (lower) phases of the QBO. Zonal winds (solid lines) in  $\text{m s}^{-1}$ ; acceleration (dashed lines) in  $\text{m s}^{-1}\text{month}^{-1}$ . [From Dunkerton and Delisi (1985). American Meteorological Society.]

Because of its long period and equatorial symmetry, the QBO in the mean zonal wind is in thermal wind balance throughout the equatorial region. For the equatorial  $\beta$ -plane this balance is given by Eq. (4.7.2), which in terms of  $\bar{T}$  may be expressed as

$$\bar{u}_z = -R(H\beta y)^{-1}\bar{T}_y. \quad (8.2.1)$$

Assuming equatorial symmetry so that  $\bar{T}_y = 0$  at  $y = 0$ , L'Hôpital's rule

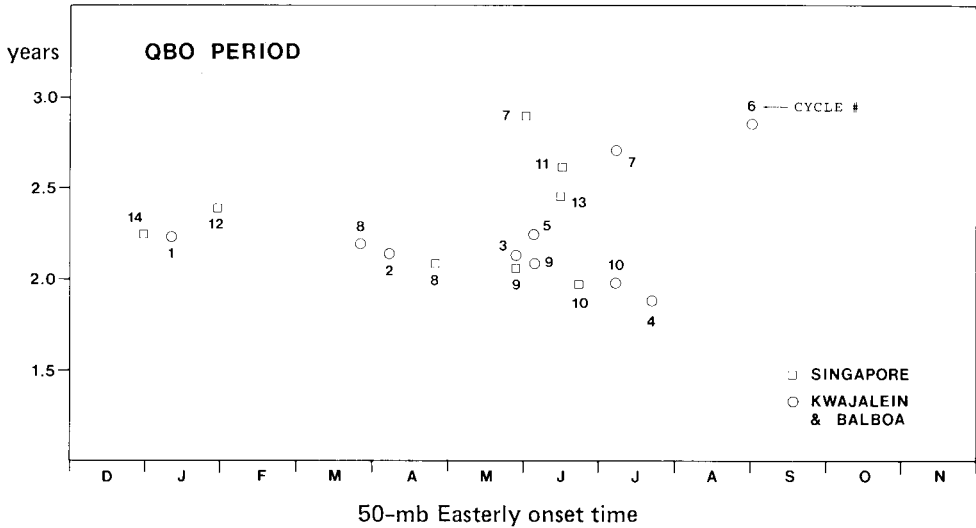


**Fig. 8.4.** Period of QBO cycles as a function of the time of easterly wind onset at the 50-mb level. Notice the clustering of easterly onset occurrences during Northern-Hemisphere summer. [Adapted by T. Dunkerton, from Dunkerton and Delisi (1985). American Meteorological Society.]

yields at the equator

$$\bar{u}_z = -R(H\beta)^{-1}\bar{T}_{yy}. \tag{8.2.2}$$

In the descending shear zones of the QBO,  $\bar{u}_z \sim 5 \text{ m s}^{-1} \text{ km}^{-1}$ , so that for a meridional scale of  $L \sim 1200 \text{ km}$  the equatorial temperature anomaly can be estimated from Eq. (8.2.2) as  $\delta\bar{T} \sim L^2 H\beta R^{-1} \bar{u}_z \sim 3 \text{ K}$ , in approximate agreement with observations. As shown qualitatively in Fig. 8.5, the westerly and easterly shear zones have warm and cold temperature anomalies, respectively. In the absence of dynamical heating or cooling, radiative relaxation would damp these anomalies with a 1- to 2-week timescale. Thus, maintenance of the thermal wind balance requires adiabatic heating (cooling) by a secondary residual meridional circulation with sinking (rising) at the equator in the westerly (easterly) shear zones as shown schematically in Fig. 8.5.

This mean meridional circulation is too weak to be directly observed. However, the vertical advection and the Coriolis torque associated with it (see Fig. 8.5) may account for some of the observed asymmetries between the easterly and westerly shear zones. The vertical advection is also consistent with the phase of the equatorial portion of the QBO observed in total ozone (Hasebe, 1983), although the QBO in ozone appears to have marked asymmetry with respect to the equator and substantial amplitude at high latitudes.

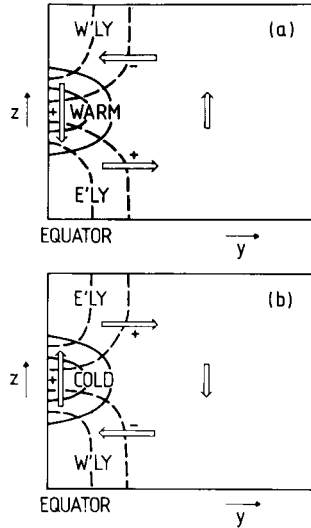


**Fig. 8.5.** Schematic latitude-height sections showing the mean meridional circulation associated with the equatorial temperature anomaly of the QBO. Solid contours show temperature anomaly isotherms, dashed contours are zonal wind isopleths. Plus and minus signs designate signs of the zonal wind accelerations driven by the mean meridional circulation. (a) Westerly shear zone, (b) easterly shear zone. [From Plumb and Bell (1982), with permission.]

This and other high latitude manifestations of the QBO will be discussed in Section 12.5.1.

### 8.3 Theory of the Quasi-Biennial Oscillation

Perhaps the three most remarkable features of the QBO that theory must explain are (1) the quasi-biennial periodicity, (2) the occurrence of zonally symmetric westerlies at the equator, and (3) the downward propagation without loss of amplitude. Early efforts to explain the periodicity were generally based on postulated biennial cycles either in the diabatic forcing in the stratosphere or in various elements of the tropospheric circulation. Aside from the fact that the observed oscillation is *not* biennial, but quite irregular in period, none of these theories could plausibly account for the structure of the observed oscillation. In particular, mechanisms based on advection by zonally symmetric inviscid circulations (which are angular-momentum-conserving) could not account for the production of a maximum in the absolute angular momentum at the equator during the westerly phase of the oscillation. Apparently zonally asymmetric wave forcing is required to explain this “superrotation.” Since it is well known that lateral momentum

transport by large-scale waves is important for the angular momentum budget of the troposphere, it was natural to suspect that planetary wave momentum fluxes might generate the quasi-biennial oscillation. However, the numerical modeling study by Wallace and Holton (1968) showed rather conclusively that lateral momentum transfer by planetary waves could not explain the downward propagation of the QBO without loss of amplitude.

The only process suggested to date that can successfully account for all three of the above-mentioned aspects of the QBO is vertical transfer of momentum by equatorial waves. A model of the QBO based on vertically propagating waves was first proposed by Lindzen and Holton (1968) and refined by Holton and Lindzen (1972, hereafter referred to as HL). HL argued that the QBO is an internal oscillation that results from the wave mean-flow interaction that occurs when vertically propagating Kelvin and Rossby-gravity waves are radiatively or mechanically damped in the lower stratosphere. The mechanism of the HL model was further elucidated by Plumb (1977), who discussed a simple analog nonrotating stratified fluid, and by Plumb and McEwan (1978), who reported an ingenious laboratory simulation of Plumb's analog to the QBO. Because it provides a simply understood prototype, it is useful to discuss Plumb's model before considering the HL model in detail.

### 8.3.1 A Two-Dimensional Analog of the QBO<sup>1</sup>

In his theoretical model, Plumb (1977) considered a vertically unbounded, nonrotating, stratified fluid subject to a standing wave forcing at its lower boundary of the form

$$\cos(kx) \cos(kct) = \frac{1}{2} [\cos k(x - ct) + \cos k(x + ct)].$$

Thus, the oscillation at the lower boundary is equivalent to two traveling waves of equal amplitude and oppositely directed phase speeds. This forcing generates vertically propagating internal gravity waves that propagate upward into the fluid, where Plumb supposed that they were dissipated by a weak Newtonian cooling with constant rate  $\alpha$ .

Assuming that the mean flow is slowly varying so that the WKB approximation is valid for the waves, the EP flux  $F^{(z)} = -\rho_0 \overline{u'w'}$  [cf. Eq. (3.5.3b)] can be expressed as

$$F^{(z)} = \sum_{i=1}^2 F_i(z) = \sum_{i=1}^2 F_i(0) \exp \left[ - \int_0^z g_i(z') dz' \right] \quad (8.3.1a)$$

where

$$g_i(z) = \alpha N [k(\bar{u} - c_i)^2]^{-1} \quad (8.3.1b)$$

<sup>1</sup> The discussion in this section follows Plumb (1984).

is just the Newtonian relaxation rate divided by the vertical component of the group velocity [see Eq. (4.6.6)]. Here  $c_1 = -c_2 = c$  and  $F_1(0) = -F_2(0)$ .

The mean flow acceleration is given by the simple one-dimensional equation

$$\frac{\partial \bar{u}}{\partial t} = \frac{1}{\rho_0} \sum \frac{\partial F_i}{\partial z} + \nu \frac{\partial^2 \bar{u}}{\partial z^2} \tag{8.3.2}$$

where  $\nu$  designates a viscosity that is assumed to act on the mean flow. When  $\bar{u} = 0$  the total EP flux vanishes for all  $z$ :  $F_1 + F_2 = 0$ , and the mean flow acceleration is zero. However, as shown by Plumb, this equilibrium is unstable for sufficiently small  $\nu$ , since if  $\bar{u}$  has a small westerly perturbation (for example), the westerly wave has lower vertical group velocity than the easterly wave and hence will be damped more rapidly, as shown in Fig. 8.6a (see Appendix 4A). Thus, a positive acceleration will occur at higher levels due to the “shielding” effect of the westerly  $\bar{u}$ . As shown in Fig. 8.6b, the initial perturbation in  $\bar{u}$  will then amplify. Plumb (1977) showed that the maximum acceleration will occur below the maximum  $\bar{u}$ , and hence the jet maximum must descend in time.

That this instability can lead to a finite amplitude mean wind oscillation resembling the QBO is shown in Fig. 8.7. As the shear zone separating the easterly and westerly regimes descends, it becomes sufficiently narrow that

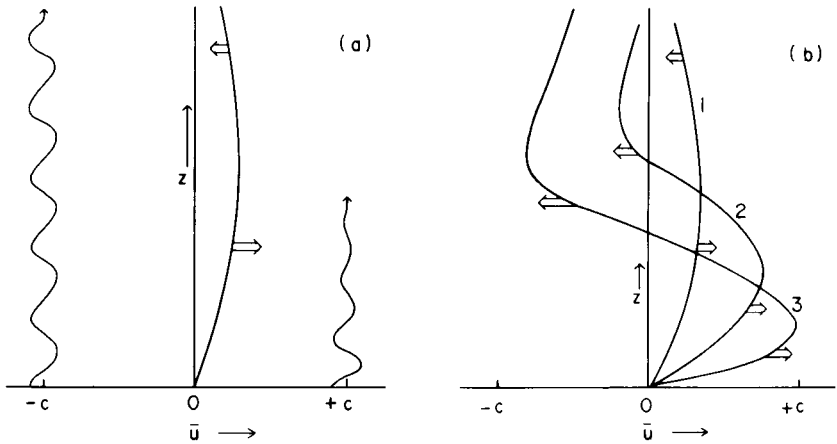


**Fig. 8.6.** Schematic representation of the instability of zonal flow in a stratified fluid with standing-wave forcing at a lower boundary. (a) Onset of instability from a small zonal flow perturbation. (b) Early stages of the subsequent mean-flow evolution. Broad arrows show locations and direction of maxima in mean wind acceleration. Wavy lines indicate relative penetration of wave components of positive and negative phase speeds  $c$ . [From Plumb (1982), with permission.]

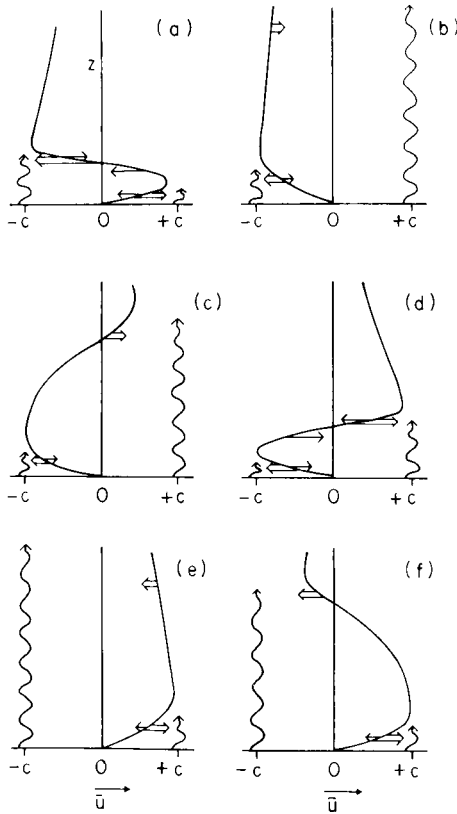


**Fig. 8.7.** Schematic representation of the evolution of the mean flow in Plumb's analog of the QBO. Six stages of a complete cycle are shown. Double arrows show wave-driven accelerations and single arrows show viscously driven accelerations. Wavy lines indicate relative penetration of easterly and westerly waves. See text for details. [After Plumb (1984).]

viscous diffusion across the shear zone destroys the low level westerlies. The westerly wave is then free to propagate to high levels through the easterly mean flow (Fig. 8.7b), where dissipation and the resulting westerly acceleration gradually build a new westerly regime that propagates downward (Figs. 8.7c,d). This in turn narrows the shear zone between the low-level easterly regime and the upper-level westerlies until diffusion destroys the easterlies (Fig. 8.7e). The easterly wave then can penetrate to high levels, where it initiates a new easterly phase of the oscillation (Fig. 8.7f). Thus, the nonlinear interaction between the mean flow and the upward-propagating dissipating waves generates a finite-amplitude oscillation in the mean flow whose period depends primarily on the amplitude of the EP flux and the vertical decay scale of the waves.

This mechanism was demonstrated in a laboratory experiment by Plumb and McEwan (1978). They used an annular vessel filled with salt-stratified water with a flexible membrane divided into a number of equal segments at the base (Fig. 8.8). This membrane was oscillated to produce a standing wave forcing that excited two vertically propagating internal gravity waves of equal but opposite horizontal phase speeds. Unlike the situation in the model described above, the waves in the experiment were dissipated by viscosity rather than Newtonian cooling. However, similar considerations apply; for a forcing exceeding some critical amplitude, the experiment generated a strong mean flow consisting of alternating downward-propagating easterly and westerly regimes. The period of the oscillation was very long compared to the period of the forced waves. This experiment provides convincing evidence that the HL mechanism contains the basic physics necessary to understand the atmospheric equatorial QBO.

### 8.3.2 The Holton and Lindzen (HL) Theory of the QBO

The eastward- and westward-propagating gravity waves in Plumb's model are symmetric and produce a mean wind oscillation with symmetric westerly and easterly phases. In the atmosphere, however, rotation introduces an important asymmetry between waves with westerly and easterly phase speeds. The Kelvin and Rossby-gravity modes have structures that are strongly dependent on the  $\beta$  effect. As described in Section 4.7, the Kelvin wave has a structure in the  $(x, z)$  plane that is identical to an eastward-propagating internal gravity wave, but has an exponential decay away from the equator. The Rossby-gravity wave, on the other hand, has a rather

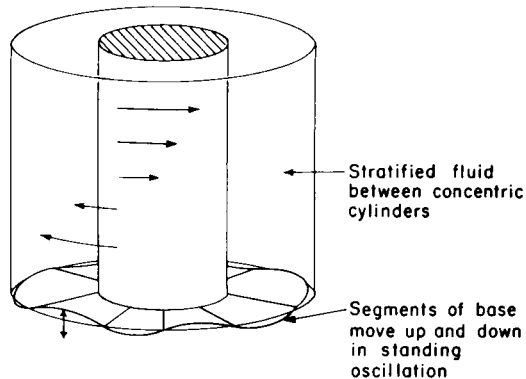


Fig. 8.8. Schematic representation of the apparatus used in the Plumb and McEwan laboratory analog of the QBO.

complex three-dimensional structure. The total effect of this wave on the mean flow cannot be assessed by examining the wave momentum fluxes alone, but rather the complete EP flux must be considered. For the Kelvin wave the EP flux is downward at each latitude, while the Rossby-gravity wave (like the Rossby wave) has an upward-directed EP flux at each latitude. Thus for waves generated in the troposphere, wave damping causes a divergence (convergence) of the latitudinally integrated EP flux for the Kelvin (Rossby-gravity) wave as illustrated in Fig. 8.9. Hence the Kelvin (Rossby-gravity) wave can in principle provide the mean zonal force necessary to generate the acceleration leading to the westerly (easterly) phase of the QBO.

In the atmosphere, unlike Plumb's model, it is necessary to account for the meridional distribution of the oscillation as well as its vertical structure. The observations reviewed in Section 4.7 indicate that observed Kelvin and Rossby-gravity waves in the equatorial lower stratosphere have meridional scales comparable to that of the zonal wind QBO. However, the latitudinal distribution of the mean wind acceleration depends on the meridional profile of the EP flux divergence. For waves damped solely by radiative relaxation (Newtonian cooling), the EP flux convergence for the Rossby-gravity wave vanishes at the equator—just where the observed acceleration is a maximum. The meridional distribution of the EP flux convergence in the Rossby-gravity wave turns out to be very sensitive to the relative magnitudes of mechanical and thermal damping and to wave transience effects. Because of the complexity of dealing theoretically with the meridional dependent mean flow, HL used a meridionally averaged model.

The HL theory is best introduced by considering the TEM version of the governing equations, Eqs. (3.5.2). For the equatorial stratosphere where  $Ri \equiv N^2/(\bar{u}_z)^2 \gg 1$  and the vertical scale for variation in  $\bar{u}$  is much greater than the vertical scale of the waves, the residual mean meridional motion ( $\bar{v}^*$ ,  $\bar{w}^*$ ) driven directly by the EP flux divergence [cf. Eq. (3.5.8)] can, to a first approximation, be neglected in Eq. (3.5.2a), which reduces then to

$$\bar{u}_t = \rho_0^{-1} \nabla \cdot \mathbf{F} + \bar{X}, \quad (8.3.3)$$

where

$$\mathbf{F} \equiv (0, F^{(y)}, F^{(z)})$$

and

$$F^{(y)} = \rho_0 [\bar{u}_z \overline{v' \theta'} / \bar{\theta}_z - \overline{u' v'}],$$

$$F^{(z)} = \rho_0 [(f - \bar{u}_y) \overline{v' \theta'} / \bar{\theta}_z - \overline{u' w'}].$$

Letting  $L$  designate the meridional scale of the QBO and noting that the QBO, the Kelvin wave, and the Rossby-gravity wave are all equatorially

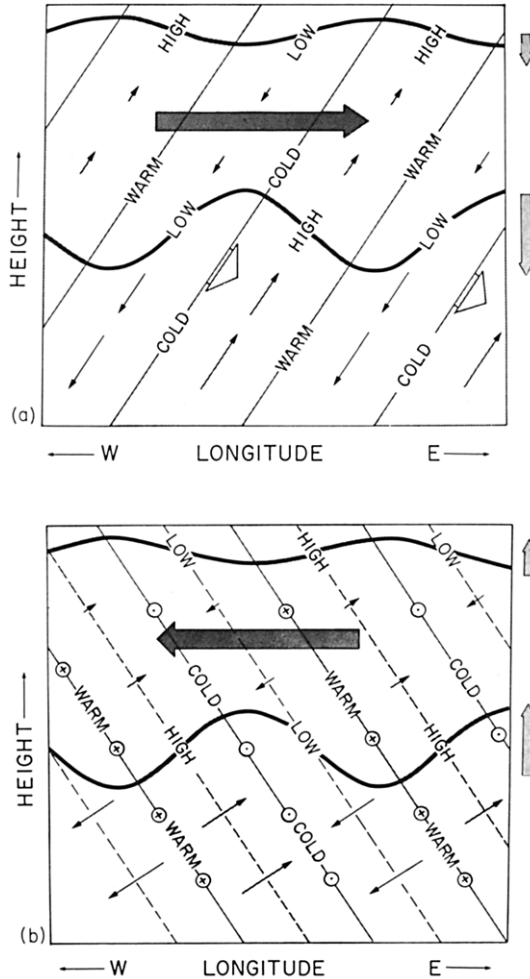


**Fig. 8.9.** (a) Longitude-height section along the equator for a thermally damped Kelvin wave; (b) longitude-height section along a latitude circle north of the equator for a thermally damped Rossby-gravity wave of westward phase speed; cf. Figs. 4.19 and 4.21. Both panels show geopotential, temperature and wind perturbations, with areas of high geopotential shaded. Heavy wavy lines indicate material surfaces, and open blunt arrows in (a) show phase propagation. Small arrows indicate zonal and vertical wind perturbations with length proportional to the wave amplitude, which decreases in height due to damping. Meridional wind perturbations are shown in (b) by arrows pointed into the page (northward) and out of the page (southward). Heavy vertical arrows to the right of the diagrams show the direction and an indication of the magnitude of the vertical component of the EP flux: this component equals the “form drag” on the indicated material surfaces (see Section 3.7.2). Heavy horizontal arrows indicate the latitudinal integral of the mean zonal force per unit mass associated with the EP flux divergence.

trapped, we may define a meridional average as follows:

$$\langle \quad \rangle \equiv \frac{1}{L} \int_{-\infty}^{+\infty} ( \quad ) dy. \quad (8.3.4)$$

Thus, since  $F^{(y)} \rightarrow 0$  as  $y \rightarrow \pm\infty$  for equatorially trapped waves, application of Eq. (8.3.4) to Eq. (8.3.3) yields

$$\langle \bar{u}_i \rangle = \rho_0^{-1} \frac{\partial}{\partial z} \langle F^{(z)} \rangle + K \frac{\partial^2 \langle \bar{u} \rangle}{\partial z^2}. \quad (8.3.5)$$

Here we have modeled  $\langle \bar{X} \rangle$  by vertical diffusion with a constant eddy viscosity  $K$ .

The wave driving is now given by the meridional average of the divergence of the vertical EP flux. In the absence of transience and damping,  $\langle F^{(z)} \rangle$  is independent of height. HL considered steady waves subject to radiative damping for which

$$\langle F^{(z)} \rangle = \sum_{i=1}^2 F_i(0) \exp \left[ - \int_0^z g_i(z') dz' \right] \quad (8.3.6)$$

with

$$g_1(z) = \alpha N [k_1(\bar{u} - c_1)^2]^{-1}$$

$$g_2(z) = \alpha N [k_2(\bar{u} - c_2)^2]^{-1} (\beta / [k_2^2(\bar{u} - c_2)] - 1).$$

Here  $i = 1$  designates the Kelvin wave and  $i = 2$  designates the Rossby-gravity wave. Comparing with Eq. (8.3.1), it is clear why Plumb's model is an analog to the HL theory.

The above expressions illustrate that some aspects of the asymmetry between easterly and westerly accelerations are retained even in a latitudinally averaged model. For both wave modes the exponential decay of the EP flux with height is proportional to the radiative damping rate divided by the vertical component of the group velocity. For the Kelvin wave the vertical group velocity is proportional to the intrinsic phase speed squared, while for the Rossby-gravity wave it is approximately proportional to the intrinsic phase speed cubed. The Kelvin wave is preferentially damped in westerly shear zones and the Rossby-gravity wave is damped in easterly shear zones. However, the latter is damped at a rate that increases more rapidly as  $(\bar{u} - c) \rightarrow 0$  than is the case for the former.

In their model calculations, HL assumed a Newtonian cooling coefficient that increased linearly from  $1/(21 \text{ days})$  at  $z = 0$  (near the 17 km level) to  $1/(7 \text{ days})$  at 30 km and remained constant above 30 km. They also assumed that at  $z = 0$  the meridionally averaged EP fluxes for the Kelvin and Rossby-gravity modes were given by

$$F_i(0)/\rho_0 = \pm 4 \times 10^{-3} \text{ m}^2 \text{ s}^{-2},$$

respectively, and that the zonal phase speeds were given by  $c_1 = -c_2 = 30 \text{ m s}^{-1}$ . The zonal wave numbers were chosen to correspond to wave number 1 for the Kelvin wave and wave number 4 for the Rossby-gravity wave, in agreement with observations. The eddy diffusion coefficient in Eq. (8.3.5) was assigned the small constant value  $0.3 \text{ m}^2 \text{ s}^{-1}$ . For this choice of parameters, Eq. (8.3.5) was integrated numerically, and the resulting time evolution of the mean zonal wind (Fig. 8.10) proved to be very similar to that of the equatorial QBO.

In this integration a semiannual cycle was imposed at the upper boundary at 35 km, but this actually has little influence on the evolution of the QBO. As Fig. 8.10 shows, the HL model generally simulates the major features of the QBO, but it does have defects. In particular, the intensity of the easterly shear zone exceeds that of the westerly shear zone, contrary to observations. This defect appears to be inevitable in the HL model, given the differing dependencies of the Kelvin and Rossby-gravity wave vertical group velocities on the intrinsic phase speed. It is conceivable that a model in which the easterly forcing were partly due to Rossby waves or to higher equatorial modes might produce the proper asymmetry. However, as shown below, a model that includes latitudinal structure can simulate the observed shear zone asymmetries, without appealing to additional easterly forcing sources.

### 8.3.3 Simulation of the Meridional Structure of the QBO

As illustrated qualitatively in Fig. 8.5, there is a secondary mean meridional circulation associated with the zonal wind and temperature

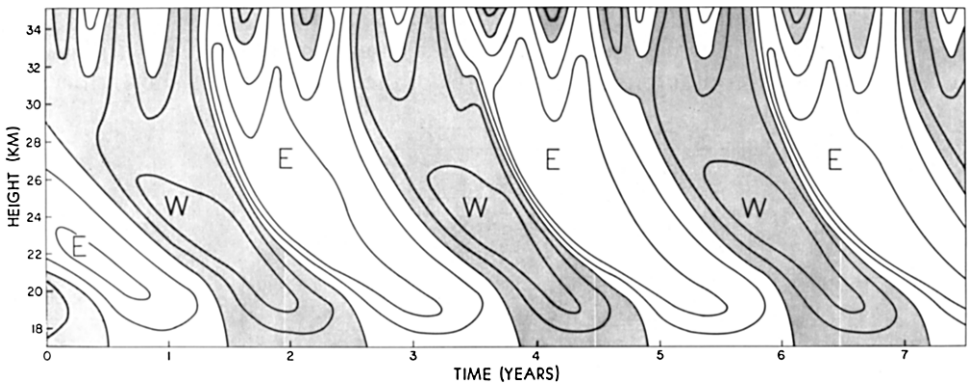


**Fig. 8.10.** Time-height section of mean zonal wind at the equator in the Holton-Lindzen model of the QBO. Contours are at  $10\text{-m s}^{-1}$  intervals, and a semiannual oscillation is imposed at the 35-km level. [From Holton and Lindzen (1972). American Meteorological Society.]

anomalies of the QBO. Although this circulation is not of primary importance to the dynamics of the basic oscillation, it should be considered in a complete theory. Near the equator the vertical advection due to the secondary circulation should tend to enhance the downward propagation of the westerly shear zone and retard the easterly shear zone. Away from the equator the Coriolis torque associated with the residual mean meridional velocity should enhance the mean wind accelerations below the main shear zone so that they are greater than the magnitudes due to the equatorial wave EP fluxes alone. Thus, it is plausible that observed shear zone asymmetries may be at least partly caused by the secondary mean meridional circulation.

The quantitative influence of the mean meridional circulation was tested by Plumb and Bell (1982). They used a two-dimensional equatorial  $\beta$ -plane model for the mean flow in which the meridional as well as the vertical distributions of  $\bar{u}$  were calculated in response to Kelvin and Rossby-gravity wave forcing. They assumed that the mean zonal wind was symmetric about the equator and that its evolution was sufficiently slow that the wave fields were at each instant adjusted to it as steady, damped waves. Thus they were able to solve for the wave fields at each instant using a numerical boundary-value technique. The resulting wave forcing was then applied to determine the EP flux divergence in the mean flow equation. Plumb and Bell formally posed their model in terms of the small amplitude version of the generalized Lagrangian mean theory (see Section 3.7). However, this is essentially equivalent to solving the TEM set [Eqs. (3.5.2)] for the equatorial  $\beta$ -plane.

Unfortunately, due to numerical stability problems, Plumb and Bell were only able to simulate a QBO of about 40% the amplitude of the observed oscillation. Despite this limitation, the Plumb and Bell model does produce a qualitatively correct shear zone asymmetry as shown in Fig. 8.11 (compare with Fig. 8.10), in which the westerly shear zone is more intense than the easterly. The overall meridional structures of the  $\bar{u}$  and  $\bar{T}$  fields shown for

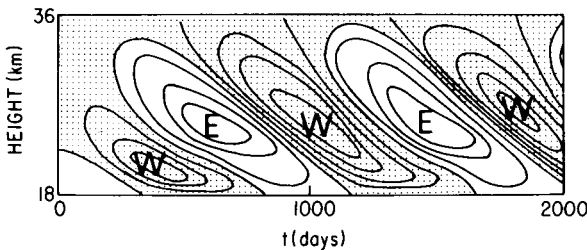
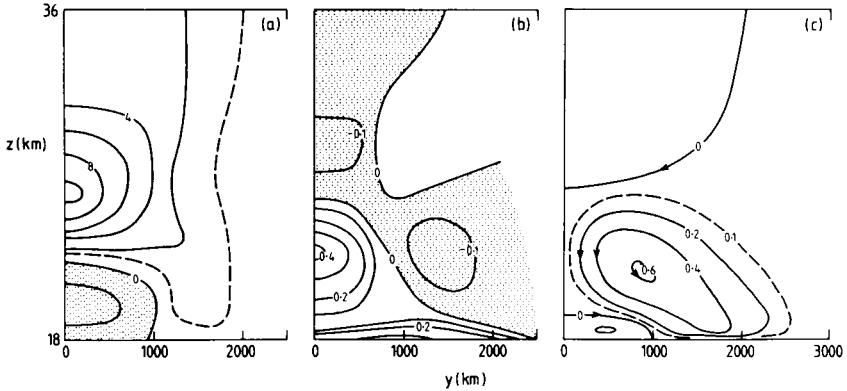


Fig. 8.11. Time-height section of mean zonal wind at the equator in the two-dimensional model of the QBO of Plumb and Bell. Contours at  $2\text{-m s}^{-1}$  intervals, easterlies are shaded. [After Plumb and Bell (1982).]



**Fig. 8.12.** Latitude–height sections showing the mean circulation at the time of the west wind maximum in the Plumb and Bell model of the QBO. (a) Zonal wind in  $\text{m s}^{-1}$ . (b) Potential temperature deviation in kelvins. (c) Mean meridional mass stream function in  $\text{m}^2 \text{s}^{-1}$ . Compare with the schematic in Fig. 8.5. [From Plumb and Bell (1982), with permission.]

the time of west wind maximum in Fig. 8.12 are also qualitatively in agreement with observations, although the meridional scale is somewhat too narrow (cf. Fig. 8.2). The mean meridional mass circulation presented in Fig. 8.12 shows, as expected, a subsidence in the shear zone near the equator and poleward drift below the shear zone. Thus vertical advection indeed speeds the westerly shear zone descent near the equator, and the Coriolis torque contributes to westerly accelerations below the shear zone away from the equator. Plumb and Bell showed that this meridional circulation quantitatively modifies the momentum budget of the QBO sufficiently to account for the computed shear zone asymmetry in their model. Since the QBO is an eddy-driven circulation, the residual meridional circulation associated with it may be regarded in a general sense as an eddy-driven circulation. But, unlike the *steady* midlatitude case discussed in Section 7.2.1, the residual circulation for the QBO is not directly determined by the EP flux divergence with the diabatic heating rate adjusting in a passive manner. Rather, the temperature change associated with the QBO determines the diabatic heating rate, which in turn helps to force the residual circulation [see Eq. (7.2.14)]. Thus, it is evident that accurate simulation of the detailed structure of the QBO depends at least to some extent on accurate calculation of the diabatic heating rates in the equatorial lower stratosphere.

Although the Plumb and Bell model does not completely reproduce all aspects of the observed QBO, it provides additional confirmation that the basic mechanism of the HL theory is valid even when the meridional

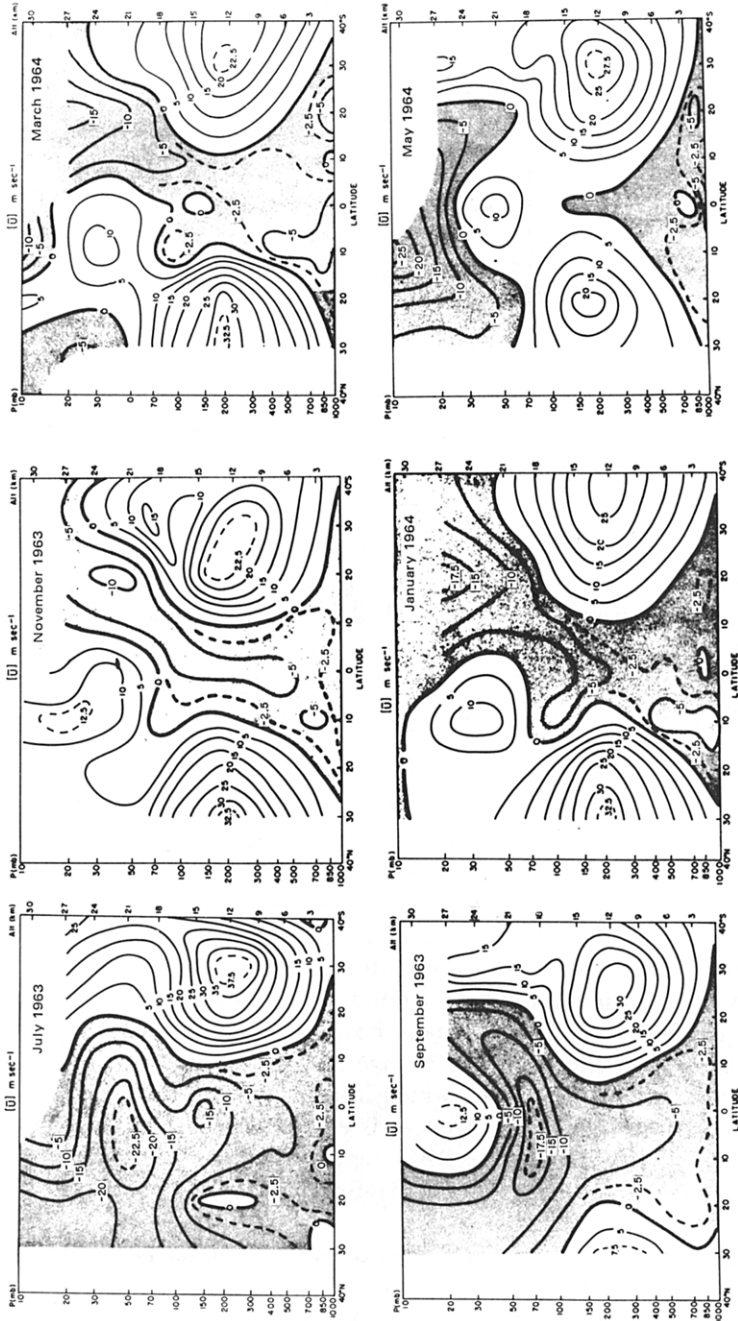


**Fig. 8.13.** Latitude-height sections showing the total mean zonal wind in the tropical region at two monthly intervals during the period July 1963 to May 1964. Notice the descending QBO westerlies and their relationship to the annual cycle. Also note the weak latitudinal shear at the equator. [From Newell *et al.* (1974), with permission.]

dependence of wave and mean-flow quantities is explicitly computed. There are, however, some important remaining problems associated with the QBO. The most significant of these is perhaps the coupling of the QBO to the annual cycle. The Plumb and Bell model assumed symmetry in the mean zonal wind about the equator. In reality, the Doppler-shifted mean flow “seen” by the Kelvin and Rossby-gravity waves is modulated by the seasonal cycle as shown in Fig. 8.13. This mean wind asymmetry will lead to some asymmetry in the vertically propagating equatorial waves, but perhaps more importantly the westerly winds of the winter hemisphere may provide ducts for the equatorward propagation of Rossby waves. Through “wavebreaking” associated with the zero mean wind critical layer, these waves may influence the QBO, as suggested by Dickinson (1968). Dunkerton (1983a) used a simple numerical model to argue that planetary waves can indeed provide part of the EP flux convergence that forces the easterly phase of the oscillation. The apparent seasonal clustering of the QBO wind reversals shown in Fig. 8.5 suggests that this sort of process may be significant. The tendency for the observed oscillation to have greater meridional width than that of the oscillation in the Plumb and Bell simulation may also be related (among other things) to the neglect of the seasonal cycle in their model.

#### 8.4 Observed Structure of the Equatorial Semiannual Oscillations

A semiannual oscillation (SAO) in the equatorial middle atmosphere was first noted by Reed (1965a) in the course of a study of the amplitude of the QBO above 30 km, as deduced from rocket soundings. Unlike the QBO, whose amplitude is a maximum in the lower stratosphere where radiosonde data are fairly plentiful, the semiannual oscillation studied by Reed is concentrated in the upper stratosphere and lower mesosphere. With the exception of the limited data set from the LIMS experiment on *Nimbus* 7, observation of this semiannual oscillation is limited to meteorological rocket temperature and wind data from relatively few locations. Zonal wind climatologies from the rocket network show that the semiannual harmonic is in fact significant not only in the tropics but at high latitudes as well (Fig. 8.14). However, the high-latitude manifestation of the semiannual harmonic appears to simply reflect a departure from sinusoidal form in the annual march of the winds.

Hirota (1978) showed that the equatorial SAO really consists of two separate oscillations centered at the stratopause and the mesopause, respectively, with an amplitude minimum near 65 km, and an approximate out-of-phase relationship between the mesopause and stratopause maxima as shown in Fig. 8.15.

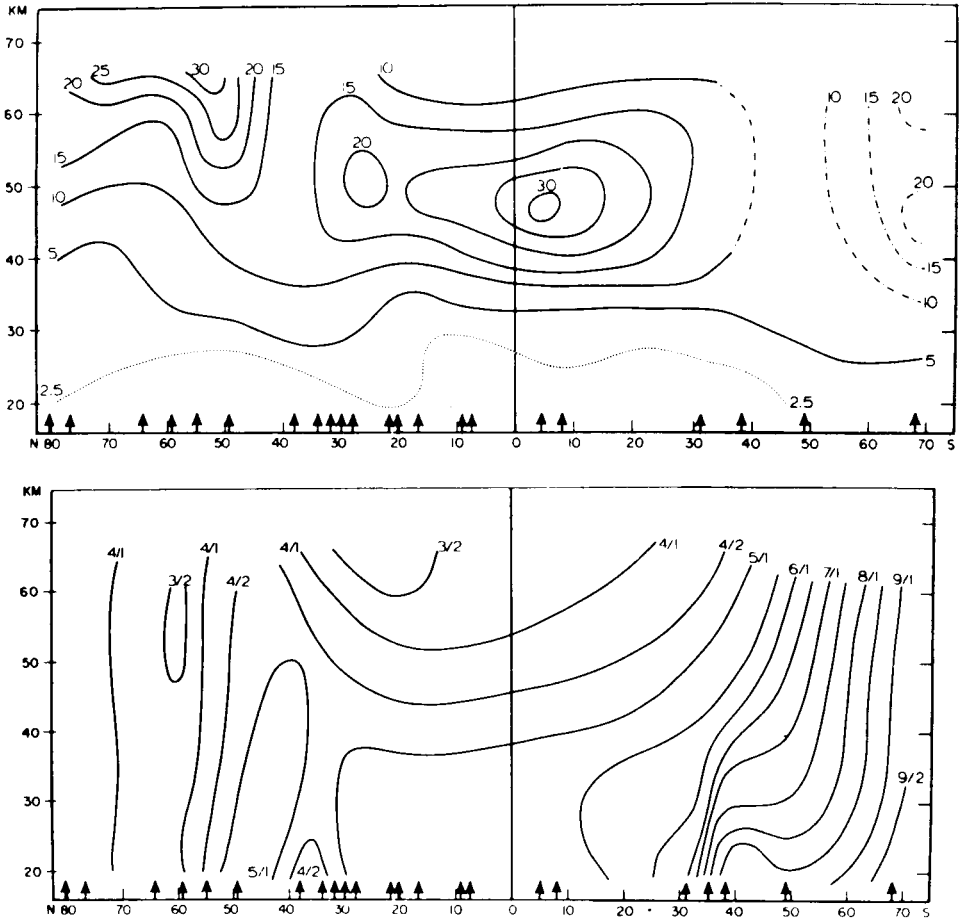
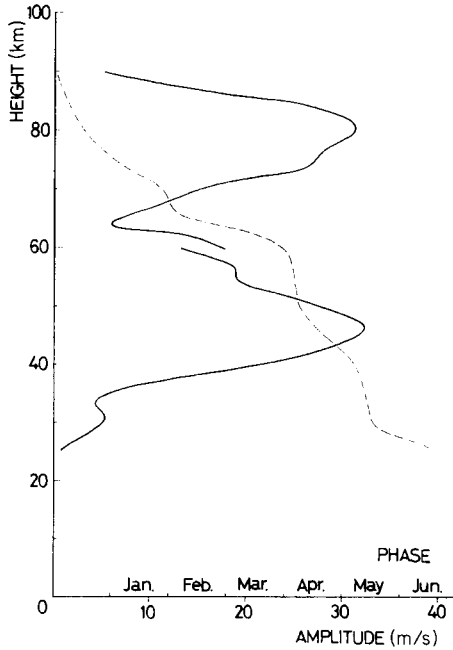


Fig. 8.14. Latitude-height sections showing the amplitude and phase of the SAO in the stratosphere and lower mesosphere. Amplitude (upper) in  $\text{m s}^{-1}$ ; phase (lower) gives date of maximum westerly component in semimonthly periods. [From Belmont *et al.*, (1974), with permission.]

The equatorial SAOs are distinct phenomena that seem to have much in common with the equatorial QBO. In particular, the oscillation centered near the stratopause has its maximum amplitude near the equator and decays away from the equator with a halfwidth of about  $25^\circ$  latitude. As indicated in Fig. 8.15, the oscillation first appears in the mesosphere and propagates downward into the stratosphere. However, the downward propagation is limited mainly to the westerly phase of the semiannual oscillation. The easterly accelerations occur nearly simultaneously over a large depth



**Fig. 8.15.** The SAO at Ascension Island ( $8^{\circ}\text{S}$ ); amplitude (solid lines), phase (dashed line). Phase refers to time of first maximum westerly component in the calendar year. Break near 60 km is caused by separately fitting data above and below that level to sinusoidal curves. [From Hirota (1978). American Meteorological Society.]

centered at the stratopause. Near the stratopause the westerly wind maxima occur at the equinoxes and the easterly wind maxima occur near the solstices. The oscillation centered at the mesopause also propagates downward, but it has its westerly wind maxima near the solstices.

## 8.5 Dynamics of the Equatorial Semiannual Oscillations

As in the case of the QBO, the semiannual oscillations centered at the stratopause and mesopause both involve generation of westerly winds at the equator and hence the production of angular momentum per unit mass greater than that of the earth. This equatorial “superrotation” cannot be explained by symmetric processes, since the observed zonal mean circulation does not indicate any region that could provide the required angular momentum. It must, therefore, be produced by eddy EP flux divergence. There is now considerable evidence that Kelvin waves provide at least a portion of the forcing for the westerly phase of the stratopause oscillation. They may

also be important for the mesopause oscillation. However, the easterly forcing is of less certain origin, and in fact may involve different mechanisms in the two height regions. For this reason, it is useful to consider the stratopause and mesopause oscillations separately.

### 8.5.1 *The Stratopause Oscillation*

Observational studies of equatorial waves show beyond doubt that the long-period Kelvin waves that are the predominant wave mode during the easterly phase of the QBO in the lower stratosphere are completely dissipated in the westerly shear zone of the QBO and cannot account for the westerly acceleration of the SAO. Holton (1975) suggested that shorter-period (high-phase-speed) Kelvin waves would experience relatively small damping in passing through the lower stratosphere, since their intrinsic phase speeds would remain large in the comparatively weak westerlies of the QBO. Thus, such waves could easily propagate into the mesosphere and drive the observed SAO.

Unfortunately, the postulated high-speed Kelvin waves were not revealed by observational analysis of lower stratospheric radiosonde data. It might be thought that due to the exponential decrease of density with height, the Kelvin-wave EP flux required to account for the westerly phase of the SAO would be an order of magnitude less than for the QBO, and that the amplitude of the high-speed Kelvin waves would thus be too small to be observable in the lower stratosphere. However, as noted by Dunkerton (1979), the timescale for the SAO is less than one-fourth that of the QBO and the amplitude is somewhat larger, so that the required EP flux at the tropopause to account for the westerly acceleration of the stratopause SAO turns out to be nearly one-third of that required for the QBO.

It is now known from rocket and satellite observations (see Section 4.7) that high-phase-speed Kelvin waves do propagate into the mesosphere. These waves appear to occur primarily in the form of transient wave “packets,” an example of which is shown in Fig. 4.27. Such packets would be difficult to detect through time-series analysis of data at a single station. The evidence from the LIMS satellite experiment suggests that Kelvin wave packets do not have sufficient amplitude to completely account for the observed westerly acceleration of the SAO [Hitchman and Leovy (1986)]. The remaining acceleration may be due to gravity-wave modes that cannot be resolved by LIMS.

The easterly phase of the stratopause SAO appears to have a primary driving mechanism that is completely different from that of the QBO. There is no evidence that the Rossby-gravity waves propagate above the lower

stratosphere. Indeed, as mentioned in Section 8.4, observations of the easterly acceleration phase of the SAO indicate nearly simultaneous accelerations over a large depth of atmosphere, contrary to the downward-propagating easterly acceleration pattern characteristic of Rossby-gravity wave absorption. The occurrence of simultaneous accelerations in a deep layer centered near the stratopause suggests that the source is meridionally propagating rather than vertically propagating.

On the basis of rocketsonde observations, Hopkins (1975) suggested that the easterly phase was driven by lateral momentum transfer due to the quasi-stationary planetary waves of the winter hemisphere. He argued that absorption of such waves in a critical layer centered at the zero mean zonal wind line in the tropics would lead to easterly accelerations that would be strongly modulated by the seasonal cycle. Thus, the SAO would result from a combination of a quasi-steady background westerly acceleration due to high-speed Kelvin-wave forcing, and a semiannually varying easterly forcing with maxima during both Northern- and Southern-hemisphere winters, and minima at the equinoctial seasons.

Holton and Wehrbein (1980) showed, however, that the residual mean meridional circulation should also be considered as a forcing for the easterly phase of the SAO. As discussed in Chapter 7 (see Fig. 7.2), the residual circulation at the solstices consists of rising motions in the summer hemisphere, a cross-equatorial drift, and sinking in the winter hemisphere; this circulation is primarily driven by eddy forcing in the extratropics. The mean meridional velocity component of this circulation is too weak in the lower stratosphere to have a significant influence. But near the stratopause, the combination of a mean meridional drift of nearly  $1 \text{ m s}^{-1}$  and a cross-equatorial mean zonal wind shear of order  $1 \text{ day}^{-1}$  implies an advective mean wind acceleration of the order of  $1 \text{ m s}^{-1} \text{ day}^{-1}$  at the equator. Thus, the simple process of advection of the summer easterlies across the equator can itself lead to a significant semiannual oscillation at the equator.

There are, however, two problems with the advective model for the easterly acceleration of the SAO. First, as shown by Holton and Wehrbein (1980), the latitudinal width of the SAO generated by mean wind advection is much less than the observed width. Second, the latitudinal velocity profiles with easterly shear at the equator are strongly inertially unstable (see Section 8.6). When the profiles are adjusted to eliminate the inertial instability, the amplitude of the resulting oscillation is reduced to less than half. Hence, it appears that mean advection alone cannot explain the easterly phase of the stratopause SAO. It is probable that both the mean advection term and planetary-wave forcing associated with vorticity mixing during wave-breaking events (see Sections 5.2.3 and 6.7) contribute to the easterly acceleration. The former may in fact enhance the latter by contributing to

the propagation of the zero mean zonal wind line into the winter hemisphere. It is important to note that these processes will both have their maximum influence during the solstices, in agreement with the observed phase of the oscillation (Fig. 8.14).

The overall model of the stratopause SAO presented here is in accord with the simulation reported by Mahlman and Umscheid (1984), who used a high-resolution general circulation model with an annually varying radiative drive. Their zonal mean wind variation at the equator (Fig. 8.16) shows a remarkably realistic stratopause SAO. Diagnosis of their model verified that the westerly accelerations were due to high-speed Kelvin waves (which are strongly excited in their model), while the easterly acceleration was due to a combination of planetary-wave forcing and mean advection.

### 8.5.2 *The Mesopause Oscillation*

Observations (Fig. 8.15) indicate a second amplitude maximum in the SAO that is not present in the simulation of Mahlman and Umscheid. Its absence in that model suggests that the oscillation may be driven by processes not simulated in the model. Dunkerton (1982b) suggested that the breaking or “saturation” of vertically propagating gravity waves might provide an explanation for the mesopause oscillation. As discussed in Section 4.6, gravity waves generated in the lower atmosphere that propagate into the mesosphere are expected to become convectively unstable and break in the mesopause region. Such waves should produce mean-flow changes due both to the resulting EP flux divergence and to wave-generated turbulent diffusion.

Dunkerton (1982b) noted that gravity-wave transmissivity through the stratopause region should be strongly modulated by the presence of the SAO, due to the strong dependence of vertical group velocity on the intrinsic frequency. Dunkerton’s mechanism is very similar to the HL model for the QBO (or, more precisely, to Plumb’s analog of the QBO discussed in Section 8.3.1). If it is assumed that gravity waves of easterly and westerly phase speeds are excited with equal intensity in the troposphere, then the westerly (easterly) waves will be preferentially radiatively damped in passing through the stratopause region during the westerly (easterly) phase of the stratopause SAO. Hence the waves that first break on reaching the mesopause region will be easterly (westerly) during the westerly (easterly) phase of the stratopause SAO. These will tend to drive easterly (westerly) accelerations, and thus there should be an approximate out-of-phase relationship between the stratopause and the mesopause oscillations, as is observed. (A somewhat similar “filtering” process was mentioned in Section 7.3.)

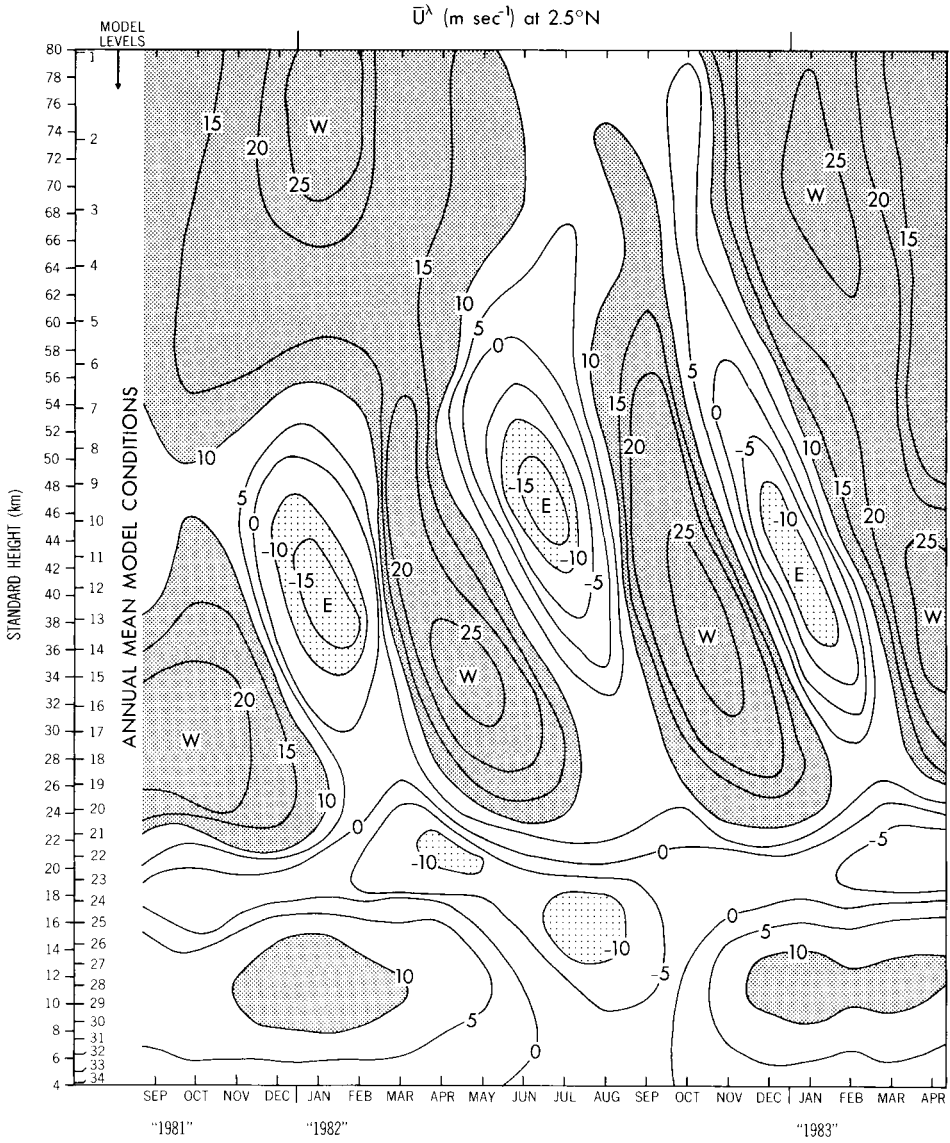


**Fig. 8.16.** Time-height cross section of monthly averaged zonal mean winds ( $m \text{ s}^{-1}$ ) at  $2.5^{\circ}\text{N}$  in the "SKYHI" general circulation model. [From Mahlman and Umscheid (1984), with permission.]

Dunkerton (1982b) pointed out that the net mean-flow driving by any process that depends on selective transmission of vertically propagating waves requires a model that includes the background winds as well as the oscillating winds, since the wave damping depends on the total intrinsic phase speed—including effects from the background mean wind. If mean wind effects are properly taken into account, then, as shown by Dunkerton (1982b), it is possible to produce a mesopause SAO approximately in accord with the observed in a model that employs Lindzen's (1981) parameterization for gravity-wave breaking as the forcing mechanism.

Dunkerton's model is suggestive, but it depends on specification of gravity-wave parameters that are not easily determined from observations (at least at present). It should also be mentioned that the extremely high-phase-speed Kelvin waves reported by Salby *et al.* (1984) may provide much of the westerly acceleration observed in the mesopause oscillation, as was pointed out by Dunkerton (1982b).

### 8.6 Inertial Instability in the Equatorial Zone

In this section we consider the possibility that the equatorial middle atmosphere may be unstable to disturbances that are almost independent of longitude. It is known (e.g., Charney, 1973) that a purely zonal basic flow  $[\bar{u}(y, z), 0, 0]$  on a  $\beta$ -plane is unstable to zonally symmetric disturbances if  $f\bar{P} < 0$  somewhere, where  $f(y)$  is the Coriolis parameter and

$$\bar{P} = \rho_0^{-1}[\bar{\theta}_z(f - \bar{u}_y) + \bar{\theta}_y\bar{u}_z]$$

is the Ertel potential vorticity of the basic state [cf. Eq. (3.1.4)]. (It is assumed that the zonal absolute angular momentum of the flow represented by  $\bar{u}$  is positive, as is always true for flows in the earth's atmosphere, except possibly near the poles.) Using the  $\beta$ -plane version of the thermal wind equation [Eq. (3.4.1c)], namely,  $f\bar{u}_z = -RH^{-1}\bar{\theta}_y e^{-\kappa z/H}$ , and the definition [Eq. (3.2.13)] of  $N^2$ , this condition for "symmetric instability" becomes

$$\bar{\theta}_z[f(f - \bar{u}_y) - f^2\bar{u}_z^2/N^2] < 0 \quad \text{somewhere,} \quad (8.6.1)$$

since  $\rho_0 > 0$ .

Two types of symmetric instability can be distinguished: *static* or *convective* instability, which occurs when  $\bar{\theta}_z < 0$  and the term in square brackets in Eq. (8.6.1) is positive, and *inertial instability*, which occurs when  $\bar{\theta}_z > 0$  but

$$f^2(1 - \text{Ri}^{-1}) - f\bar{u}_z < 0 \quad \text{somewhere,} \quad (8.6.2)$$

where  $\text{Ri} \equiv N^2/\bar{u}_z^2$  is the Richardson number. This condition can be shown to be equivalent to the statement that the absolute angular momentum per

unit mass on an isentrope decreases with radial distance from the axis of rotation. Inertial instability arises from an imbalance between the pressure gradient force and the total centrifugal force, and is closely analogous to the more familiar convective instability, which arises from an imbalance between the pressure gradient force and the buoyancy force. For barotropic flow ( $\bar{u}_z = 0$  or  $Ri = \infty$ ), the criterion may be expressed as  $f(f - \bar{u}_y) < 0$ . Thus (unless  $\bar{u}_y = 0$  and  $\beta - \bar{u}_{yy} > 0$  at  $y = 0$ ) a zonally symmetric barotropic flow will be inertially unstable somewhere near the equator. For baroclinic flows with  $Ri < 1$ , Eq. (8.6.2) shows that instability can occur even without meridional shear. For the zonally averaged circulation of the equatorial middle atmosphere,  $Ri \gg 1$  in general so that baroclinic effects can be neglected. However, although observations (Fig. 8.13) indicate that in the lower stratosphere the meridional shear of the mean zonal wind is very small near the equator, in the upper stratosphere and mesosphere this may not be the case. In this region the cross-equatorial advection by the mean circulation will tend to produce a cross-equatorial shear by advecting the summer-hemisphere easterly flow toward the winter hemisphere. Thus, the mean circulation will tend to produce an inertially unstable zonal-mean flow profile. The study of inertial instability in the equatorial middle atmosphere is, therefore, not merely of academic interest.

An example of inertial instability can be derived from the linear disturbance equations for the equatorial beta-plane discussed in Section 4.7. Following Dunkerton (1981a), we set  $\partial/\partial x = 0$ ,  $X' = Y' = Q' = 0$  (so that disturbances are zonally symmetric and conservative), and  $\bar{u} = \bar{u}(y)$  in Eqs. (4.7.1); by Eq. (4.7.2),  $\bar{\theta}_y = 0$  also. Then it is readily verified that the meridional velocity disturbance satisfies

$$\frac{d^2 \hat{v}}{dy^2} + \frac{m^2}{N^2} [\omega^2 - \beta y (\beta y - \bar{u}_y)] \hat{v} = 0. \quad (8.6.3)$$

This may be reduced to the canonical form of Eq. (4.7.13c) if, following Boyd (1978a), we assume that the mean wind shear is linear:  $\bar{u}_y = \gamma$ , and shift latitude by letting

$$y_1 = y - \gamma(2\beta)^{-1}$$

and define

$$\omega_1^2 = \omega^2 + \gamma^2/4. \quad (8.6.4)$$

Then Eq. (8.6.3) becomes equivalent to Eq. (4.7.13c) provided we let

$$\eta = (\beta|m|/N)^{1/2} y_1,$$

and the eigencondition relating  $\omega_1$  and  $m$  is

$$m^2 \omega_1^2 / N^2 = (2n + 1) \beta |m| / N \quad (8.6.5)$$

[cf. Eq. (4.7.15)]. Thus for the lowest mode ( $n = 0$ ) the frequency  $\omega$  corresponding to a disturbance of wave number  $m$  is given from Eqs. (8.6.4) and (8.6.5) as

$$\omega^2 = N\beta/|m| - \gamma^2/4. \quad (8.6.6)$$

For  $N\beta/|m| < \gamma^2/4$  the frequency  $\omega$  is imaginary and approaches an asymptotic value of  $\pm i\gamma/2$  as  $|m| \rightarrow \infty$ . Recalling that the perturbation solution was assumed to have a dependence of the form  $\exp[i(mz - \omega t)]$ , we see that the positive root corresponds to an exponentially growing mode.

For inertial instability, like convection, the fastest-growing mode has infinitesimal scale (i.e.,  $|m| \rightarrow \infty$  in the present case). In the atmosphere it is expected that eddy diffusion will damp the smallest scales so that the maximum growth rate will occur for a finite scale. Dunkerton (1981a) showed that inertially unstable modes have only a weak dependence on the magnitude of the assumed eddy viscosity. (The critical shear for marginal instability depends on the  $\frac{1}{2}$  power of the viscosity coefficient, and the critical vertical scale goes as the  $\frac{2}{3}$  power.) For a vertical viscosity coefficient of  $1 \text{ m}^{-2} \text{ s}^{-1}$ , marginal instability requires a meridional shear of  $\sim 2.8 \text{ day}^{-1}$  and the corresponding lowest mode has vertical wavelength of 2.4 km and meridional scale of  $5.25^\circ$  latitude. Just as convection transfers heat vertically, thereby tending to eliminate static instability, inertially unstable modes transfer momentum meridionally and thus should tend to reduce the lateral shear until the profile is marginally stable. The structure of the resulting lowest-order neutral viscous mode is shown qualitatively in Fig. 8.17. The aspect ratio (vertical/meridional scale) depends weakly on eddy diffusion, so that the ellipses flatten out as viscosity approaches zero.

A structure suggestive of inertial instability has been identified in the LIMS satellite radiance data (Hitchman *et al.*, 1987). This vertically stacked “pancake” pattern in the meridional and zonal velocity fields has also been simulated in the general circulation model of Hunt (1981). The absence of such structure in the model of Holton and Wehrbein (1980) is presumably due to the fact that their model lacked sufficient vertical resolution to resolve the small vertical scales that would characterize inertial instability for the magnitude of damping in the model.

More work is required to determine the true role of inertial instability in the equatorial middle atmosphere. The theory presented here involves *zonally symmetric* disturbances to a *zonally symmetric* basic state. Large-amplitude Kelvin waves are often present in the equatorial easterlies so that the “basic state” zonal flow is *not* zonally symmetric. Furthermore, the disturbances observed by LIMS that have been interpreted as inertial instabilities are also *not* zonally symmetric. There is some theoretical evidence that zonally asymmetric inertial instabilities may occur in the

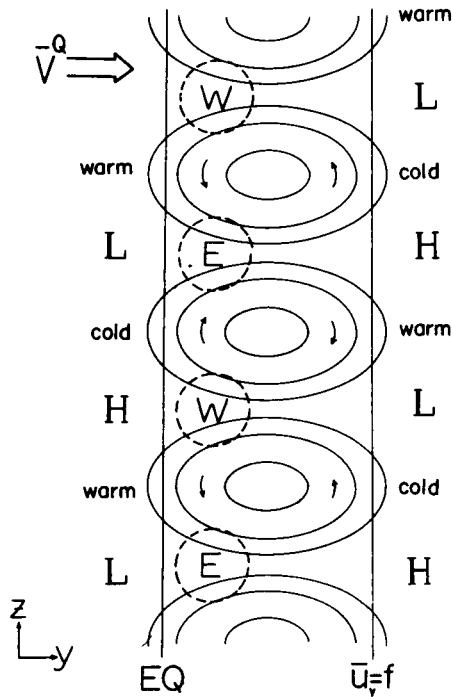


**Fig. 8.17.** Schematic representation of the lowest order neutral viscous inertial mode on the equatorial  $\beta$ -plane. The residual circulation  $\bar{v}^Q$  generates an inertially unstable region between the equator and the latitude where  $f = \bar{u}_y$ . The elliptical contours indicate the perturbation motion in the meridional plane, and the dashed contours indicate the maxima in the induced perturbation zonal flow. The pressure anomalies are indicated by the symbols L and H for low and high pressures, respectively. [After Dunkerton (1981a). American Meteorological Society.]

presence of a zonally symmetric basic state (Boyd and Christidis, 1982; Dunkerton, 1983b). But the relevance of these theoretical calculations to the atmosphere is uncertain. Nevertheless, present evidence suggests that inertial instability could be an important mechanism for limiting the magnitude of lateral wind shear in the equatorial zone and thereby reducing the mean wind acceleration due to advection by the residual circulation.

## References

8.1. Observed seasonal and longer term variations in the lower stratosphere are discussed in detail by Newell *et al.* (1974). Thermal forcing in the equatorial zone is considered by Wallace (1967) and Wallace and Holton (1968).

8.2. Observational studies of the QBO are reviewed by Reed (1965b), Wallace (1973), and Plumb (1984), all of whom provide references to many original sources. Detailed analyses of the observed meridional structure of the QBO are contained in Dunkerton and Delisi (1985) and Hamilton (1984).

8.3. The theory of the QBO is reviewed in the excellent survey by Plumb (1984). Briefer accounts are given by Holton (1983b) and Andrews (1985). The vertical structure is discussed by Hamilton (1981b), the role of wave transience by Dunkerton (1981b). The meridional dependence of Kelvin and Rossby-gravity wave EP flux divergence are discussed by Andrews and McIntyre (1976a,b), Boyd (1978b), and Holton (1979b). Dunkerton (1985) discusses a two-dimensional model of the QBO.

8.4. Observational evidence for the SAO is reviewed by Hirota (1980), who provides references to original sources. The mesospheric SAO is discussed by Hamilton (1982c).

8.5. Theoretical aspects of the SAO are discussed in a series of papers by Dunkerton (1979, 1982a,b). A two-dimensional numerical model is reported by Takahashi (1984). Hamilton (1986) uses a diagnostic model to infer the nature of the distribution of the forcing of the SAO.

8.6. Symmetric inertial instability in the equatorial zone is discussed by Dunkerton (1981a) and by Stevens (1983). Symmetric instability in a more general context is treated by Emanuel (1979).